



TECHNICAL ARTICLE

# Feasibility of the Use of Gas Phase Inhibition of Hydrogen Embrittlement in Gas Transmission Pipelines Carrying Hydrogen: A Review

ANDREJ ATRENS <sup>1,3</sup> EVAN GRAY,<sup>2</sup> JEFFREY VENEZUELA,<sup>1</sup>  
JOSHUA HOSCHKE,<sup>1</sup> and MAXIMILIAN ROETHIG<sup>1</sup>

1.—School of Mechanical and Mining Engineering, Centre for Advanced Materials Processing and Manufacturing (AMPAM), The University of Queensland, St. Lucia, QLD, Australia.  
2.—Queensland Micro- and Nanotechnology Centre, Griffith University, Brisbane 4111, Australia.  
3.—e-mail: andrejs.atrens@uq.edu.au

This review paper introduces a research project that seeks to quantify oxygen inhibition of gaseous hydrogen embrittlement with possible application for gas transmission pipelines transporting hydrogen. And it summarizes the compelling laboratory evidence that oxygen may inhibit gaseous hydrogen embrittlement. Quantification of oxygen inhibition of gaseous hydrogen embrittlement is needed to allow evaluation of this approach to the inhibition of hydrogen embrittlement in gas transmission pipelines. The experimental approach is explained as the quantification of the amount of hydrogen entering the steel from gas mixtures containing hydrogen using a purpose-built gas phase permeation cell.

## INTRODUCTION

Compelling laboratory evidence indicates that O<sub>2</sub> can inhibit the environment hydrogen embrittlement (EHE) of the steels of gas transmission pipelines carrying hydrogen gas. Other gases (CO, CO<sub>2</sub>) have also been shown to cause inhibition of EHE. The proposed oxygen concentration ([O] ≤ 1000 vppm) is allowed by Australian Standard AS 4564:2020 *General-purpose natural gas*, and is lower than that which would cause burning, and is lower than that produced by a typical hydrogen electrolyser.

If 100% inhibition of EHE were practical, then the mechanical behavior of the steel remains unchanged. The operating characteristics would remain the same. Nevertheless, the use of this inhibition strategy requires in-depth understanding, particularly because thermodynamics indicates that the inhibition is a kinetic effect.

The research project RP3.1-13 funded by the Future Fuels Cooperative Research Centre, Australia, proposes (1) to study the hydrogen flux entering gas transmission pipeline steels exposed to hydrogen and hydrogen methane mixtures (at partial pressures from 1 to 200 bar hydrogen) in the presence of small amounts of up to 1% of added gases, such as O<sub>2</sub>, CO, and CO<sub>2</sub>; and (2) to study how the hydrogen concentration approaches the equilibrium hydrogen solubility in the gas transmission pipeline steels, in particular how quickly equilibrium is approached depending on (1) the hydrogen fugacity, (2) the presence of surface oxide on the steel surface, and (3) the presence in the hydrogen gas in small amounts of up to 1% of the added gases such as O<sub>2</sub>, CO, and CO<sub>2</sub>.

## LITERATURE SUMMARY

### Gas-Phase Inhibition of Environment Hydrogen Embrittlement (EHE)

Surface inhibition of hydrogen entry into steel causes the hydrogen concentration to slowly approach the equilibrium hydrogen solubility, so that environment hydrogen embrittlement (EHE) is inhibited for tests in gaseous hydrogen containing a

small amount of a gas (such as O<sub>2</sub>, CH<sub>4</sub>, CO, CO<sub>2</sub>), e.g., as shown in Refs. 1, 2. Holbrook et al.<sup>1</sup> showed that the fracture toughness of X42 and X70 pipeline steels measured in hydrogen gas was significantly lower than in N<sub>2</sub>, but was essentially the same as in N<sub>2</sub> when measured in hydrogen containing CO. Holbrook et al.<sup>1</sup> attributed the inhibition to (1) the blocking of sites on the steel surface and, consequently, (2) the inhibition of hydrogen absorption into the steel. Furthermore, the blocking of surface sites was reported to be not 100%.

Holbrook et al.<sup>1</sup> indicate that this is a kinetic effect inhibiting hydrogen entry. That is, the speed of hydrogen entry is decreased by the inhibiting gases. This means that the hydrogen concentration will nevertheless reach the equilibrium concentration with time, whereupon the steel mechanical properties will be determined by the equilibrium hydrogen concentration. Furthermore, a gas transmission pipeline has a long lifetime (> 50 years), so equilibrium may be expected to occur. However, it is not known how quickly equilibrium is approached. If the inhibition would substantially decrease the amount of hydrogen in the steel over the pipe lifetime, then this inhibition is a possible practical strategy to control EHE. However, detailed in-depth understanding is required.

Oxygen in hydrogen gas also inhibits hydrogen-facilitated fatigue crack growth.<sup>3</sup> The frequency dependence of the fatigue crack growth rate<sup>3</sup> of X52 gas pipeline steel at  $\Delta K \sim 21 \text{ MPa}\sqrt{\text{m}}$  in 21 MPa hydrogen, with the stated oxygen concentrations compared with fatigue crack growth in air ( $\Delta K$  is the magnitude of the change of the stress intensity factor,  $K$ ), is presented in Fig. 1. At 10 Hz, these oxygen concentrations did not decrease the fatigue crack growth rate, as the fatigue crack growth rate was the same as in pure hydrogen. However, at 1 Hz, 100 volume parts per million (vppm) O<sub>2</sub> and 1000 vppm O<sub>2</sub> decreased the fatigue crack growth rate to the fatigue crack growth rate in air, and, at

0.1 Hz, 10 vppm O<sub>2</sub> was sufficient to decrease the fatigue crack growth rate to the fatigue crack growth rate in air. This indicated that the oxygen inhibition became more effective as the frequency was decreased.<sup>3</sup>

This increased oxygen inhibition effectiveness with decreasing frequency is the exact opposite to what is usually measured in hydrogen embrittlement studies. Usually, hydrogen embrittlement becomes more severe with decreasing load frequency when there is more time for hydrogen to diffuse to the crack tip and cause embrittlement. Figure 1 shows the exact opposite,<sup>3</sup> instead showing increasing inhibitor effectiveness with decreasing frequency, which allows more time for hydrogen diffusion. In this case, the increased inhibitor effectiveness with decreasing frequency was explained by the adsorption of oxygen at the fresh surface produced by each fatigue cycle. For the slower frequency, there was more time for the oxygen to adsorb on the freshly created fatigue surface, and so a smaller oxygen concentration was needed in the gas phase.<sup>3</sup>

Fracture toughness tests data for American Society of Testing and Materials (ASTM) A333 grade 6 pipe steel in hydrogen with the stated oxygen concentrations are presented in Fig. 2 in terms of the  $J$  integral and crack extension,  $\Delta a$ . The fracture toughness in hydrogen containing 100 vppm oxygen was the same as the fracture toughness in air, indicating complete inhibition by the 100 vppm oxygen. The  $J$  integral– $\Delta a$  curve in hydrogen containing 10 vppm oxygen was between the curve in air and the curve in hydrogen containing less than 0.1 vppm, indicating partial inhibition by 10 vppm oxygen.

The fractography and crack tip shape<sup>4</sup> supported the conclusion that 100 vppm oxygen inhibition was by the preferential adsorption of oxygen on the steel

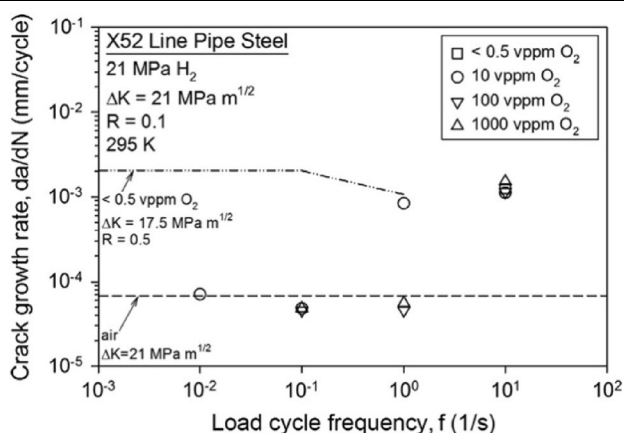


Fig. 1. Frequency dependence of fatigue crack growth<sup>3</sup> of X52 gas pipeline steel at  $\Delta K \sim 21 \text{ MPa}\sqrt{\text{m}}$  in 21 MPa hydrogen with the stated oxygen concentrations, compared with fatigue crack growth in air. Reprinted with permission from Ref. 3.

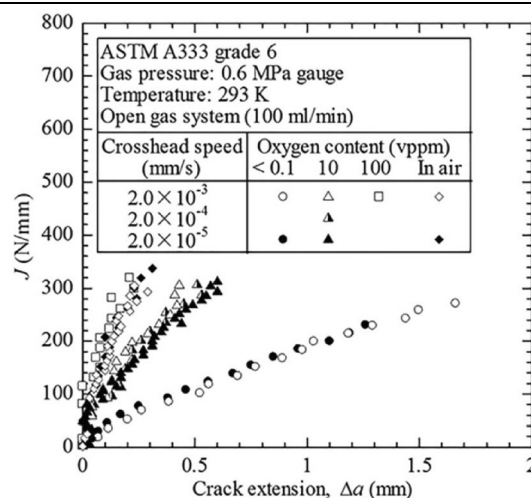


Fig. 2. Fracture toughness tests of ASTM A333 grade 6 pipe steel in hydrogen with the stated oxygen concentrations. Reprinted with permission from Ref. 4.

surface at the crack tip, and that the preferential adsorption prevented EHE by the prevention of hydrogen entry into the steel. The crack tip shape for the J-integral tests in air indicated crack tip blunting (Fig. 3a). The crack tip was similarly blunted in  $H_2$  with 100 vppm  $O_2$  (Fig. 3c). In contrast, the crack remained sharp in  $H_2$  with 0.1 vppm  $O_2$  (Fig. 3b). There was some blunting in  $H_2$  with 10 vppm  $O_2$ , consistent with the higher fracture toughness compared with in  $H_2$  with 0.1 vppm  $O_2$  (Fig. 3d).

Gas phase inhibitor effectiveness was studied theoretically by Staykov et al.<sup>5</sup> using density functional theory modeling. Catalytic dissociation of the hydrogen molecule,  $H_2$ , into two H atoms, occurred at the steel surface, overcoming an activation barrier of 0.1 eV. This hydrogen molecule dissociation is a necessary step for hydrogen atoms to enter the steel from the gaseous hydrogen. In contrast, there was no activation barrier for oxygen molecule dissociation on a clean Fe surface.<sup>5</sup> Furthermore, the attractive force on the oxygen molecule by the Fe surface was found to be substantially larger than on the hydrogen molecule, suggesting a higher oxygen concentration close to the Fe surface, so that a continuous coverage of the surface by oxygen was expected. Moreover, hydrogen molecules were repelled from the Fe surface already covered with dissociated oxygen, so that the hydrogen molecules did not dissociate and so could not enter the steel. This research<sup>5</sup> implied that the oxygen inhibition of EHE could be 100%, but this research did not explicitly make the claim of 100% inhibition.

This provides compelling laboratory evidence that small amounts of  $O_2$  can inhibit the EHE of gas transmission pipelines carrying hydrogen gas. The key question is the inhibition effectiveness. Inhibition effectiveness determines how much hydrogen enters the steel despite the oxygen inhibition, and the rate of approach to equilibrium hydrogen solubility in the steel in the presence of effective oxygen inhibition.

## Newly Designed Permeation Cell to Study Inhibition Effectiveness

The effectiveness of oxygen blocking of hydrogen entry into the steel can be assessed by directly measuring the amount of hydrogen entering the steel from the gas phase, using the newly designed permeation cell, as illustrated in Fig. 4 in association with the newly designed gas phase rig. This cell is similar to the hybrid cell depicted by Zhao et al.,<sup>6</sup> except that the hydrogen permeation flux is measured from the increase in pressure in the downstream part of the cell. This permeation cell allows measurement of the hydrogen flux entering the specimen from hydrogen gas, by measuring the hydrogen flux passing through the specimen and entering the detection cell downstream of the specimen. This permeation cell also allows measurement of (1) hydrogen entry from hydrogen gas containing a gas phase inhibitor like  $O_2$ , and (2) the hydrogen solubility in the steel.

## Hydrogen Solubility

Typical hydrogen solubility in steel is shown in Fig. 5. The equilibrium hydrogen concentration is shown at room temperature, measured using gaseous hydrogen charging for hydrogen pressures from 1 to 200 bar for 3.5NiCrMoV steel,<sup>7</sup> 980DP steel, and MS1500 steel,<sup>8,9</sup> and compared with literature values for annealed pure iron, designated as Fe.<sup>10</sup> The gas phase hydrogen charging of the 3.5NiCrMoV steel<sup>7</sup> required activation of the steel at 200 °C at 200 bar hydrogen to remove the surface oxide to allow hydrogen entry. The heat treatment of the 3.5NiCrMoV steel includes austenitization, quenching to form martensite, followed by tempering at a temperature substantially above  $\sim 600$  °C, so that the activation at 200 °C was unlikely to change the microstructure, including the number and types of hydrogen traps, which was confirmed by the subsequent analysis using thermal desorption spectroscopy (TDS).<sup>7</sup>

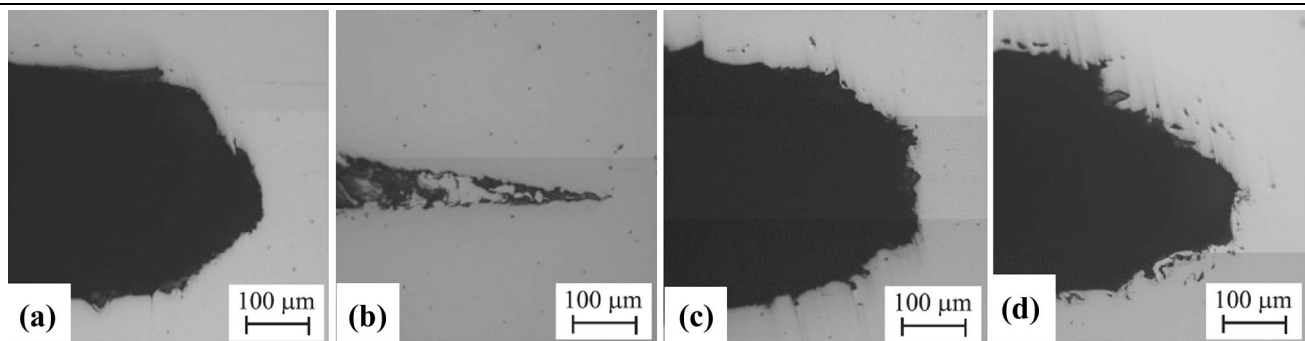


Fig. 3. (a). Crack tip shape in air; crack extension  $\Delta a = 0.25$  mm. (b) Crack tip shape in  $H_2$  with 0.1 vppm  $O_2$  and  $\Delta a = 1.66$  mm. (c) Crack tip shape in  $H_2$  with 100 vppm  $O_2$ ;  $\Delta a = 0.21$  mm. (d) Crack tip shape in  $H_2$  with 10 vppm  $O_2$  and  $\Delta a = 2.04$  mm. Reprinted with permission from Ref. 4.

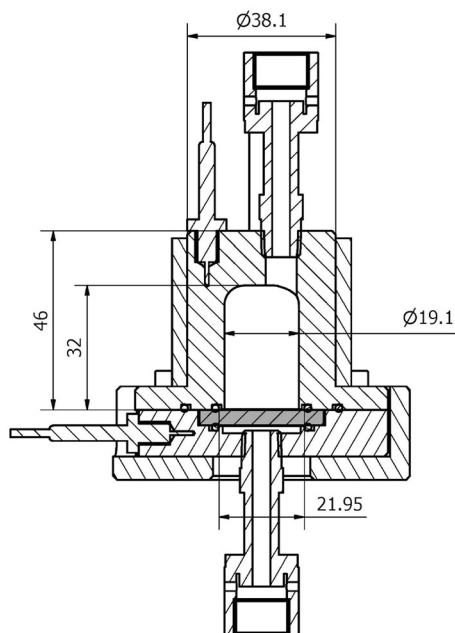


Fig. 4. Schematic of a gas phase permeation cell, capable of charging pressures of 200 bar at 200 °C. Hydrogen charging from the gas phase can use pure hydrogen, or hydrogen containing up to 1% of added gases, such as O<sub>2</sub>, CO, CH<sub>4</sub>, and CO<sub>2</sub>. The permeation membrane is shown in gray. Hydrogen charging occurs from the hydrogen gas above the steel membrane, hydrogen diffuses through the membrane, and the flux of hydrogen diffusing through the steel membrane is detected.

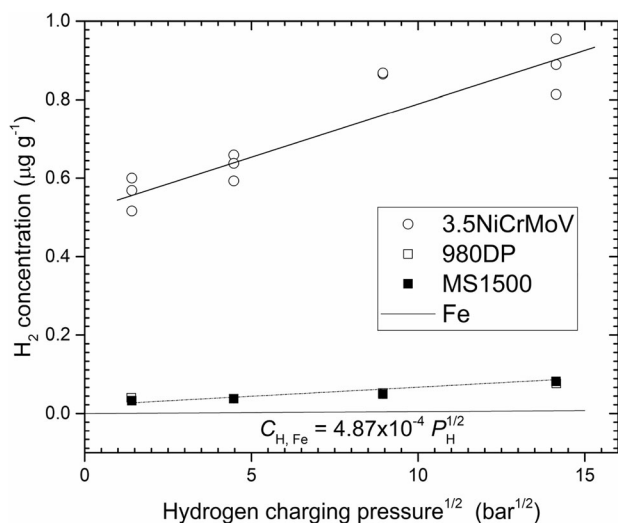


Fig. 5. Hydrogen concentration in 3.5NiCrMoV steel, 980DP, and MS1500 for various pressures of gaseous hydrogen from 1 to 200 bar at room temperature, measured using gaseous hydrogen charging,<sup>7-9</sup> compared with literature data for annealed pure Fe.<sup>10</sup> Note that the data points for 980DP are partially or completely covered by the data points for MS1500.

The hydrogen solubility in steels follows Sieverts' Law. The hydrogen concentration,  $C_{H,e}$ , in the steel is given by:

$$C_{H,e} = C_{H,T} + S(P_H)^{0.5} \quad (1)$$

where  $C_{H,T}$  is the concentration of hydrogen in hydrogen traps in the steel,  $P_H$  is the (partial) pressure of the gaseous hydrogen, and  $S$  is Sieverts' constant for the steel. Hydrogen traps are microstructural features, such as dislocations, carbide precipitates, and grain boundaries. Hydrogen in the trap sites is more tightly bound than in a normal lattice site. Hydrogen traps increase the amount of hydrogen in the steel, as is clear for the higher solubilities in the steels compared with annealed pure Fe in Fig. 5, which also shows that the hydrogen concentration in the MS1500 was 0.08 weight parts per million (wtppm) at a gaseous hydrogen pressure of 200 bar. The chemical composition of MS1500 (0.19 wt.% C, 0.35 wt.%Si, 1.51 wt.%Mn, 0.01 wt.%S, 0.01 wt.%P, 0.04 wt.%Al, 0.01 wt.%Nb, 0.03 wt.%Ti, 0.03 wt.%Cr) is similar to that of pipe line steels. Gas transmission pipelines in Australia have operating pressures of 100 or 150 bar.

Sieverts' Law can be derived using statistical mechanics, as shown in Venezuela et al.<sup>7</sup> assuming: (1) the hydrogen in the steel is in equilibrium with the hydrogen in the gas phase, (2)  $N_H$  hydrogen atoms occupy  $N_S$  sites in the steel lattice of which  $N_t$  are trap sites, and (3) only one hydrogen atom can occupy each of the  $N_S$  sites. Thus, Eq. 1 is based on thermodynamics. The equilibrium hydrogen solubility depends only on the hydrogen partial pressure in the gas and the nature of the steel (which includes the number of trap sites). No kinetic factors are involved in Eq. 1. In equilibrium, there is no influence of the presence of other gases such as O<sub>2</sub>, CO, and CO<sub>2</sub>. Moreover, the hydrogen solubility data of Fig. 5 is in good agreement with Eq. 1. There are no kinetic effects. There are no surface effects.

### Natural Gas Specification

The oxygen concentration ( $[O] \leq 1,000$  vppm) is lower than the specified limits in natural gas in Australia and the UK. The Australian Standard AS 4564:2020 General-purpose natural gas<sup>11</sup> specifies 0.2 mol.% as the maximum oxygen concentration. A similar oxygen limit of 0.2 mol.% is set in Western Australia,<sup>12,13</sup> and for the National Grid UK.<sup>14</sup> The Australian Energy Market Operator Gas Quality Guidelines<sup>15</sup> indicates that action is only required if the oxygen concentration exceeds the somewhat smaller limit of 0.15 mol.%.

### Oxygen Content in Electrolyser Hydrogen

Sharbanee<sup>16</sup> indicated that hydrogen electrolyzers demonstrate safe operational experience involving the presence of trace oxygen within hydrogen gas streams. Several examples are provided here with reference to one representative electrolyser original equipment manufacturer, Siemens Energy.

The Siemens Silyzer 300 hydrogen electrolyser specification is > 99.71 vol.% (dry basis) for



hydrogen. The impurity percentage (0.29 vol.%) is oxygen. This electrolyser has been installed overseas and has been operating safely since 2019.

The earlier Siemens model, the Silyzer 200, is the electrolyser that was installed and commissioned earlier this year at AGIG's HyP site in Tonsley, South Australia. The Silyzer 200 has a purity spec in the range 99.5–99.9 vol.% (99.5 vol.% at 40% part load). This indicates a safe working experience with up to 0.5 vol.% oxygen for hydrogen produced by an electrolyser, both in Australia, since 2021, and overseas, since 2015.

## Burning

Burning of natural gas (or hydrogen) can occur<sup>17</sup> for a natural gas concentration (or a hydrogen concentration) in air by volume between limits designated as the lower flammability limit ( $L_{EL}$ ) and the upper flammability limit ( $U_{EL}$ ). The lower flammability limit defines the minimum concentration of the flammable gas that burns. Below this limit, the gas mixture is too lean to burn. The upper flammability limit defines the maximum concentration that burns. Above this limit, there is too much flammable gas and too little oxygen. The mixture is too rich.

For methane:  $L_{EL} = 5$  v%,  $U_{EL} = 15$  v%; for hydrogen:  $L_{EL} = 4$  v%,  $U_{EL} = 75$  v%.<sup>17</sup>

Burning of the gas mixture can occur if too much oxygen is mixed with natural gas or mixed with hydrogen. The maximum oxygen concentration can be evaluated from the  $U_{EL}$  for natural gas or for hydrogen. The  $U_{EL}$  for hydrogen indicates that there is no burning for an oxygen concentration up to  $\sim 5$  v%. Similarly, there is no burning for methane–oxygen mixtures of considerably higher oxygen concentrations. Thus, oxygen concentrations required for burning are much larger than the oxygen limits specified for natural gas in Australia and the UK.

## RESEARCH APPROACH

The literature summarized above indicates that trace oxygen concentrations have been shown to inhibit EHE of steels in gaseous hydrogen in laboratory experiments. There is strong evidence of inhibition of the hydrogen acceleration of fatigue crack growth of pipeline steels,<sup>3</sup> and of inhibition of the hydrogen decrease of fracture toughness for a pipe steel.<sup>4</sup> There is strong evidence that this inhibition by oxygen is caused by strong preferential adsorption of oxygen at the steel surface, which has the tendency to prevent hydrogen entry into the steel, so that the hydrogen content in the steel is low.

It is also clear that the hydrogen solubility in steels is governed by Sieverts' Law. This is a thermodynamic relationship, with no effect of kinetics. The hydrogen solubility in equilibrium depends

only on the hydrogen pressure and the nature of the steel. There is no room for inhibition by oxygen under equilibrium conditions.

It is also clear that a gas pipeline is expected to have a long lifetime, greater than 50 years, so there is a lot of time for equilibrium conditions to be established.

Oxygen present in the hydrogen gas inhibits hydrogen entry into the steel from the hydrogen gas.

This inhibition can be directly measured using a gas phase permeation cell, shown schematically in Fig. 4, in conjunction with a gas phase handling arrangement.

Using pure hydrogen on the charging side, the permeation cell allows measurement of permeation transients at hydrogen pressures from 1 to 200 bar, and for temperatures from 25 to 200 °C. This allows easy measurement of hydrogen solubility and the hydrogen diffusion coefficient for all these conditions, which represent equilibrium conditions. This establishes the hydrogen flux through the steel membrane for conditions of charging using pure hydrogen.

Thereafter, it is possible to study the influence of oxygen in the hydrogen on the hydrogen flux. This allows the study of the inhibition effectiveness of oxygen in gaseous hydrogen mixtures. The goal is to be able to determine the hydrogen content in the gas pipeline steel after 50 years of pipeline operation. This hydrogen content needs to be maintained much less than 1 wtppm over the pipeline lifetime (50 years) to prevent hydrogen acceleration of fatigue crack growth and hydrogen-influenced fracture.

The permeation cell shown in Fig. 4 will be used to:

- (1) Measure the equilibrium solubility of hydrogen in the gas transmission pipeline steels, as a function of hydrogen partial pressure from 1 to 200 bar hydrogen, in hydrogen and hydrogen methane mixtures in the presence of small amounts of up to 1% of added gases, such as O<sub>2</sub>, CO, and CO<sub>2</sub>.
- (2) Study the hydrogen flux entering the steel and the approach to equilibrium solubility of hydrogen in the gas transmission pipeline steels, in particular how quickly equilibrium is approached, depending on the hydrogen fugacity and the concentration of small amounts of up to 1% of the added gases such as O<sub>2</sub>, CO, and CO<sub>2</sub>.

## Measurement of Equilibrium Hydrogen Solubility

The gas phase charging rig will allow equilibrium hydrogen gas phase charging of a steel specimen in equilibrium with hydrogen at a partial pressure from 1 to 200 bar hydrogen, in hydrogen and

hydrogen methane mixtures in the presence of small amounts of up to 1% of added gases such as O<sub>2</sub>, CO, and CO<sub>2</sub>. The hydrogen charging chamber is designed to allow for heating up to 200 °C at pressure, while the steel is being equilibrated with the hydrogen gas. This feature has been incorporated to allow for specimen activation. Thereafter, the specimen can be slowly cooled to room temperature to ensure that the hydrogen in the specimen is in equilibrium with the hydrogen gas in the chamber at room temperature. The hydrogen concentration in the specimen can then be measured using the TDS at Griffith University.<sup>18</sup> This procedure allows for the measurement of the equilibrium solubility of hydrogen in the gas transmission pipeline steels, as a function of hydrogen partial pressure from 1 to 200 bar hydrogen in hydrogen and hydrogen methane mixtures in the presence of small amounts of up to 1% of added gases such as O<sub>2</sub>, CO, and CO<sub>2</sub>. Independent measurement of the hydrogen solubility in the steel is enabled by the permeation cell (Fig. 4).

The effect of heating to 200 °C is unlikely to change the density and type of traps present in the gas pipeline steels because of the metallurgy of these steels, such as X52, X65, and X70.<sup>19–24</sup> To ensure cost-effectiveness, these steels are micro-alloyed and thermo-mechanically processed when austenitic, such that there is significant hot working at temperatures and such that the precipitates of the micro-alloying elements restrict austenite grain growth, ensuring a small resulting grain size of the ferrite and pearlite microstructure and good mechanical properties. The metallurgical transformations of the austenite into essentially equilibrium microconstituents ensure a stable microstructure, which does not change significantly if reheated to 200 °C.

These measurements of hydrogen solubility will be carried out for the gas pipeline steels used for the hydrogen embrittlement studies at the University of Queensland (UQ) and The University of Wollongong.

#### Outputs

- Equilibrium solubility of hydrogen in the gas transmission pipeline steels at room temperature as a function of hydrogen partial pressure from 1 to 200 bar hydrogen, in hydrogen and hydrogen-methane mixtures in the presence of small amounts of up to 1% of added gases such as O<sub>2</sub>, CO, and CO<sub>2</sub>, for the gas pipeline steels used for the hydrogen embrittlement studies at UQ.
- It is expected that the equilibrium solubility of hydrogen in the gas transmission pipeline steels at room temperature depends purely on the hydrogen partial pressure from 1 to 200 bar hydrogen,
- It is expected that there is little effect on the equilibrium hydrogen solubility of small

amounts of up to 1% of added gases, such as O<sub>2</sub>, CO, and CO<sub>2</sub>.

#### Approach to Equilibrium Hydrogen Solubility

The gas phase permeation cell presented in Fig. 4 will be used to study the approach to equilibrium solubility of hydrogen in the gas transmission pipeline steels, in particular the hydrogen flux entering the steel and how quickly equilibrium hydrogen solubility is approached, depending on the hydrogen concentration and the concentration of small amounts of up to 1% of the added gases such as O<sub>2</sub>, CO, and CO<sub>2</sub>. The effect of an initial surface oxide will also be studied. This gas phase permeation cell has been designed to measure hydrogen permeation through the steel specimen charged with gas phase hydrogen. Thus, we will determine the hydrogen solubility and diffusivity in the pipeline steels at temperatures between room temperature and 200 °C. The gas phase permeation cell will also be used to study the inhibition of hydrogen entry into the gas pipeline steel by the presence of the gases such as O<sub>2</sub>, CO, and CO<sub>2</sub>, and thus inhibition will be studied.

#### Outputs

- Hydrogen solubility and diffusivity in the pipeline steels at temperatures between room temperature and 200 °C as measured using the permeability cell. This provides an independent cross-check on the hydrogen solubility measured by the TDS.
- An understanding of the inhibition of hydrogen entry into gas pipeline steels by the presence of the gases such as O<sub>2</sub>, CO, and CO<sub>2</sub>.
- An understanding of the possibility of an interaction between an initial surface oxide and gas phase oxygen inhibition of EHE.
- It is expected that the hydrogen solubility follows an Arrhenius-type relationship with temperature, and that the hydrogen solubility at room temperature measured with the permeation cell is equal to that measured by gas phase charging of specimens.
- It is expected that inhibition of hydrogen entry at 200 °C is minor, so that hydrogen equilibrium solubility is approached rapidly and the speed of approach to equilibrium decreases with decreasing temperature.
- The inhibition experiments at 200 °C will lend credence to the results at lower temperatures.
- The hydrogen diffusivity evaluations will include the evaluation of the hydrogen diffusivity of steel containing no hydrogen. The initial diffusivity is expected to be low as the hydrogen traps are filled. These measurements will allow assessment of the practical significance of the expected initial lower hydrogen diffusivity as the hydrogen traps are filled.

## ACKNOWLEDGEMENTS

This research has been supported by the Future Fuels Cooperative Research Centre project RP3.1-13. Sam Grieve is thanked for his design of the permeability cell and his assistance in the design and construction of the gas mixing rig.

## FUNDING

Open Access funding enabled and organized by CAUL and its Member Institutions.

## CONFLICT OF INTEREST

The authors declare that they have no conflict of interest.

## OPEN ACCESS

This article is licensed under a Creative Commons Attribution 4.0 International License, which permits use, sharing, adaptation, distribution and reproduction in any medium or format, as long as you give appropriate credit to the original author(s) and the source, provide a link to the Creative Commons licence, and indicate if changes were made. The images or other third party material in this article are included in the article's Creative Commons licence, unless indicated otherwise in a credit line to the material. If material is not included in the article's Creative Commons licence and your intended use is not permitted by statutory regulation or exceeds the permitted use, you will need to obtain permission directly from the copyright holder. To view a copy of this licence, visit <http://creativecommons.org/licenses/by/4.0/>.

## REFERENCES

1. J.H. Holbrook, H.J. Cialone, E.W. Collings, E.J. Drauglis, P.M. Scott, and M.E. Mayfield, Control of hydrogen embrittlement of metals by chemical inhibitors and coatings, in *Gaseous Hydrogen Embrittlement of Materials in Energy Technologies*. (Elsevier, Amsterdam, 2012), pp. 129–153. <https://doi.org/10.1533/9780857095374.1.129>.
2. K. Xu, Hydrogen embrittlement of carbon steels and their welds, in *Gaseous Hydrogen Embrittlement of Materials in Energy Technologies*. (Elsevier, Amsterdam, 2012), pp. 526–561. <https://doi.org/10.1533/9780857093899.3.526>.
3. B.P. Somerday, P. Sofronis, K.A. Nibur, C.S. March, and R. Kirchheim, *Acta Mater.* 61, 6153 (2013).
4. R. Komoda, M. Kubota, A. Staykov, P. Ginet, and F. Barbier, *Fatigue Fract. Eng. Mater. Struct.* 42, 1387 (2019).
5. A. Staykov, J. Yamabe, and B.P. Somerday, *Inter. J. Quant. Chem.* 114, 626 (2014).
6. W. Zhao, T. Zhang, Y. Zhao, J. Sun, and Y. Wang, *Corros. Sci.* 111, 84 (2016).
7. J. Venezuela, C. Tapia-Bastidas, Q. Zhou, T. Depover, K. Verbeken, E. Gray, Q. Liu, Q. Liu, M. Zhang, and A. Atrens, *Corros. Sci.* 132, 90 (2018).
8. J. Venezuela, E. Gray, Q. Liu, Q. Zhou, C. Tapia-Bastidas, M. Zhang, and A. Atrens, *Corros. Sci.* 127, 45 (2017).
9. Q. Liu, E. Gray, J. Venezuela, Q. Zhou, C. Tapia-Bastidas, M. Zhang, and A. Atrens, *Adv. Engin. Mater.* 20, 1700469 (2018).
10. K. Kiuchi and R.M. McLellan, *Acta Metall.* 7, 961 (1983).
11. Austr. Standard AS 4564:2020, *Standards Austr.* (2020).
12. W. A. Gas Supply (Gas Quality Spec.) Act 2009, Gas Supply (Gas Quality Spec.) Reg. 2010, Version 01-b0-02, [www.legislation.wa.gov.au](http://www.legislation.wa.gov.au).
13. M. Soltik, *Economic Regulation Authority*, W. A., (2007).
14. <https://www.nationalgrid.com/UK/gas-transmission/data-and-operations/quality>, Accessed 6 Sept 2021.
15. Aus. Ener. Market Oper. AEMO, Gas Qual. Guide., (2017).
16. S. Sharbanee, Tech. Man. – Ener. Syst., Enscope A Quanta Services Co., private comm.s 3 & 14 Sept 2021.
17. J.G. Speight, *Handbook of natural gas analysis* (Wiley, Hoboken, 2018).
18. C.V. Tapia-Bastidas, A. Atrens, and E.M. Gray, *Int. J. Hyd. Ener.* 43, 7600 (2018).
19. J.Q. Wang and A. Atrens, *J. Mater. Sci.* 38, 323 (2003).
20. J.Q. Wang, A. Atrens, and D.R. Cousens, *J. Mater. Sci.* 34, 1711 (1999).
21. J.Q. Wang, A. Atrens, D.R. Cousens, and N. Kinaev, *J. Mater. Sci.* 34, 1721 (1999).
22. J.Q. Wang, A. Atrens, D.R. Cousens, P.M. Kelly, C. Nockolds, and S. Bulcock, *Acta Mater.* 46, 5677 (1998).
23. D.R. Cousens, B.J. Wood, J.Q. Wang, and A. Atrens, *Surf. Inter. Anal.* 29, 23 (2000).
24. A. Atrens, J.Q. Wang, K. Stiller, and H.O. Andren, *Corros. Sci.* 48, 79 (2006).

**Publisher's Note** Springer Nature remains neutral with regard to jurisdictional claims in published maps and institutional affiliations.